

## Rhythmic Network Modulation to Thalamocortical Couplings in Epilepsy

Yun Qin\*, Nan Zhang\*, Yan Chen\*, Xiaojun Zuo\*, Sisi Jiang\*,  
Xiaole Zhao\*, Li Dong\*, Jianfu Li\*, Tao Zhang\*,  
Dezhong Yao\*<sup>†</sup> and Cheng Luo\*<sup>†,‡</sup>

*\*The Clinical Hospital of Chengdu Brain Science Institute  
MOE Key Lab for Neuroinformation  
High-Field Magnetic Resonance Brain Imaging Key Laboratory of Sichuan Province  
University of Electronic Science and Technology of China  
Chengdu 610054, P. R. China*

*<sup>†</sup>Research Unit of NeuroInformation, Chinese Academy of Medical Sciences  
2019RU035, Chengdu, P. R. China  
<sup>‡</sup>chengluo@uestc.edu.cn*

Accepted 21 January 2020  
Published Online 18 April 2020

Thalamus interacts with cortical areas, generating oscillations characterized by their rhythm and levels of synchrony. However, little is known of what function the rhythmic dynamic may serve in thalamocortical couplings. This work introduced a general approach to investigate the modulatory contribution of rhythmic scalp network to the thalamo-frontal couplings in juvenile myoclonic epilepsy (JME) and frontal lobe epilepsy (FLE). Here, time-varying rhythmic network was constructed using the adapted directed transfer function between EEG electrodes, and then was applied as a modulator in fMRI-based thalamocortical functional couplings. Furthermore, the relationship between corticocortical connectivity and rhythm-dependent thalamocortical coupling was examined. The results revealed thalamocortical couplings modulated by EEG scalp network have frequency-dependent characteristics. Increased thalamus-sensorimotor network (SMN) and thalamus-default mode network (DMN) couplings in JME were strongly modulated by alpha band. These thalamus-SMN couplings demonstrated enhanced association with SMN-related corticocortical connectivity. In addition, altered theta-dependent and beta-dependent thalamus-frontoparietal network (FPN) couplings were found in FLE. The reduced theta-dependent thalamus-FPN couplings were associated with the decreased FPN-related corticocortical connectivity. This study proposed interactive links between the rhythmic modulation and thalamocortical coupling. The crucial role of SMN and FPN in subcortical-cortical circuit may have implications for intervention in generalized and focal epilepsy.

*Keywords:* Thalamocortical coupling; corticocortical connectivity; rhythmic scalp network; modulation; epilepsy.

---

<sup>‡</sup>Corresponding author.

## 1. Introduction

Thalamus subserves cognitive functions by interacting with cortical and other subcortical areas.<sup>1</sup> Thalamocortical circuit has the intrinsic capacity to generate different types of oscillations with their rhythm and levels of synchrony.<sup>2</sup> Specifically, thalamocortical couplings contribute to initiating and stabilizing cortical connectivity among brain areas.<sup>3</sup> The interactions between thalamocortical and corticocortical circuit give rise to dynamic information regulation according to behavioral demands.<sup>4,5</sup> Nonetheless, these interactions are as yet insufficiently investigated with the knowledge of large-scale connectivity, and little is known of what modulatory function the cortical synchronized organization may serve in thalamocortical couplings.

Oscillation regularities and the optimal synchronization operation of cortical activity enable healthy brains to sustain homeostasis in processing exteroceptive or interoceptive information.<sup>6</sup> Synchronization within local neural network and interactions between regions integrate the information and were supposed to be the basis of perception.<sup>7</sup> The dynamic regulation by complex homeostatic processes has been specifically and sensitively detected by scalp EEG with different frequency bands, reflecting the sequence of synchronized activity in huge neural ensembles with spatiotemporal patterns.<sup>8–10</sup> While, shifts from this stable self-organization can be induced in many neurological and psychiatric disorders.<sup>11–14</sup>

Aberrant neural oscillation and cortical synchrony has been demonstrated in epilepsy,<sup>15,16</sup> such as abnormal individual alpha frequency, and the altered intrinsic connectivity of certain rhythm.<sup>17–19</sup> Moreover, evidence has indicated the implications of subcortical-cortical connectivity relating to epilepsy.<sup>20–22</sup> Current concepts postulated thalamocortical loops played an important role in epileptic discharge generation.<sup>23</sup> Corticocortical couplings were suggested facilitating the discharge propagation.<sup>24,25</sup> A lot of methodology has been provided for seizure detection based on different scale of neural and functional network concept.<sup>26–30</sup> Juvenile myoclonic epilepsy (JME), as a common subtype of idiopathic generalized epilepsy (IGE), was characterized by 2–6 Hz generalized spike-wave or polyspike wave discharges (GSWD) with a frontocentral predominance.<sup>31,32</sup> In EEG recording of frontal lobe

epilepsy (FLE), interictal epileptiform discharges were obviously observed in frontal electrodes. Similar large area of frontal cortex was involved both in JME and FLE; however, distinct network representations were described. Sensorimotor network (SMN) was one important network in JME, and the hyperconnectivity within SMN was widely considered acting as the excitatory driver in discharge propagation.<sup>33</sup> While in FLE, increased local spatiotemporal consistency was found in the frontoparietal network (FPN).<sup>34</sup> In addition, another frontal-related network, the default mode network (DMN) was more likely to reveal spike-triggered blood oxygenation level-dependent (BOLD) deactivation both in IGE and FLE.<sup>35,36</sup> This heterogeneity of the network representations was puzzling, and we hypothesized that the dynamic organization of rhythmic network may contribute to this diversity, in the context of the thalamus-mediated mechanism.

BOLD-fMRI measures changes of the blood oxygenation level in brain circuits, and it can provide maps of brain metabolic activity and dynamic configuration of brain network.<sup>37–39</sup> Previous study showed that fMRI activity might represent the localized changes in neuronal synchrony without increasing firing-rate.<sup>40–42</sup> Coupling between fMRI and local field potential (LFP), as well as the scalp signals based on EEG or magnetoencephalography (MEG) was also demonstrated.<sup>43–46</sup> However, there has been no data available linking the cortical global synchronization represented in EEG and the long-range spatial circuit represented in fMRI. EEG-fMRI fusion provided a valid approach to search for the haemodynamic correlations with the ongoing neuronal rhythmic oscillation, linking the EEG oscillation with the whole brain, even the deep sub-cortical structures. However, the relationship between rhythm features and epilepsy-related functional connectivity in the brain is still not very clear. Especially, the thalamocortical circuit modulated by the EEG dynamics cross frequency and time needs to be investigated in detail for better understanding the pathophysiology of epilepsy.

In this study, we focus on the role of brain rhythmic dynamic in functional connectivity across certain thalamocortical circuits, including thalamus-SMN, thalamus-FPN, and thalamus-DMN couplings. We have two basic hypotheses: first, the thalamocortical coupling was modulated by rhythmic network;

second, this modulation can be altered in epilepsy; furthermore, JME and FLE may show common and distinct modulatory effects. Based on simultaneous EEG-fMRI data, time-varying network organization of different frequency band was constructed using adapted directed transfer function (ADTF) between EEG electrodes. Then, a psychophysiological interaction (PPI) framework<sup>47,48</sup> was applied to link thalamocortical couplings and the rhythmic networks, which provided a linear regression framework to detect the coupling of one region to another with the modulation of other experimental or intrinsic factors. Furthermore, the associations between corticocortical connectivity among networks and rhythm modulatory thalamocortical couplings were examined.

## 2. Methods

### 2.1. Participant

Two groups of epilepsy patients were recruited in this study, including 21 JME patients (12 females; mean age  $\pm$  standard deviation (SD):  $21 \pm 7$  years)

and 17 FLE patients (10 females; mean age  $\pm$  SD:  $23 \pm 11$  years). The patients were diagnosed by neurologists based on the clinical and seizure semiology information according to International League Against Epilepsy (ILAE) guidelines.<sup>49,50</sup> No structural abnormality was observed by routine CT and MRI examinations for JME and FLE patients. Table 1 showed the demographic variables of the two epilepsy groups. A total of 20 healthy controls (5 females; mean age  $\pm$  SD:  $24 \pm 4$  years) with no history of neurologic or psychiatric disorders participated in this study. All participants gave written informed consent in accordance with the Declaration of Helsinki. This study was performed based on the guidelines approved by the Ethics Committee of the University of Electronic Science and Technology of China (UESTC).

### 2.2. Simultaneous EEG-fMRI recording

In this study, simultaneous EEG-fMRI recordings were collected for all participants in UESTC. MRI

Table 1. Detailed demographic information and clinical characteristics of JME and FLE patients.

JME						FLE					
No.	Age (year)	F/M	Age of onset	AEDs	Avg No. of Seizures	No.	Age (year)	F/M	Age of onset	AEDs	Avg No. of Seizures
1	17	F	10	VPA	1	1	7	F	1	TPM	2
2	17	F	14	LTG	1	2	24	M	16	CBZ	4
-3	33	F	20	VPM	3	3	23	F	16	LTG	0.5
4	22	M	8	VPM	2	4	22	F	12	TPM	0
5	19	F	12	MgV	1	5	42	M	38	TPM	0
6	20	F	6	VPM/LTG	6	6	14	F	3	CBZ	0
7	15	M	5	—	4	7	15	F	11	—	0
8	22	F	14	VPA	2	8	13	F	10	OXC	1
9	17	F	3	VPA	0.5	9	27	M	10	VPM/PIR	0.1
10	17	F	13	VPA	0.5	10	25	M	8	CBZ	0
11	29	F	10	TCM/VPM	5	11	32	F	18	VPA	0.5
12	18	M	14	VPM	1	12	16	F	7	LEV	1
13	27	F	16	—	3	13	28	F	18	CBZ	5
14	21	F	11	VPM	0.5	14	14	M	11	OXC	0
15	10	M	5	VPM	1	15	31	F	3	VPA/TPM	1
16	13	M	9	VPA	4	16	51	M	9	—	15
17	34	M	14	TCM/VPM	5	17	20	M	10	VPA	1
18	34	F	18	—	1						
19	28	M	17	VPA	5						
20	18	M	7	OXC/TPM	10						
21	23	M	13	VPM	0.5						

Note: No.: number; AEDs: Antiepileptic drugs; VPA: valproic acid; LTG: lamotrigine; VPM: valpromide; OXC: oxcarbazepine; TPM: Topamax; CBZ: carbamazepine; PIR, piracetam; LEV, levetiracetam; MgV: magnesium valproate; TCM, traditional Chinese medicine. F/M: Female/Male; Avg No. of Seizures: averaged number of seizures per month.

data were acquired using a 3-T MRI scanner (Discovery MR750, GE) in the Center for Information in Medicine of UESTC. Resting state fMRI data were acquired using the gradient-echo echo planar imaging sequences (FOV =  $24 \times 24 \text{ cm}^2$ , FA =  $90^\circ$ , TR/TE = 2000 ms/30 ms, matrix =  $64 \times 64$ , slicethickness/gap = 4 mm/0.4 mm), with an eight channel-phased array head coil. A total of 255 volumes were collected in the resting-state scan for each participant. In addition, high-resolution T1-weighted images were also acquired using a three-dimensional fast spoiled gradient echo (T1-3D FSPGR) sequence (FOV =  $25.6 \times 25.6 \text{ cm}^2$ , FA =  $9^\circ$ , matrix =  $256 \times 256$ , TR/TE = 5.936 ms/1.956 ms, slicethickness = 1 mm, no gap, 152 slices).

For all participants, simultaneous EEG data were recorded using a MR compatible EEG cap (64-channel, Neuroscan, Charlotte, NC) according to the 10–20 standard system. The amplifier was settled outside the scanning room and the sampling rate was 5000 Hz. The recording reference was set at the Fcz position, and electrode impedances were lowered to below  $10 \text{ k}\Omega$  before recording. Synchronization between EEG recording and the MR internal clock was conducted to facilitate the artifacts removal in EEG preprocessing. During the simultaneous recording, all participants were instructed to remain still and close their eyes without sleeping.

### 2.3. EEG-fMRI data preprocessing

fMRI data were preprocessed using SPM12 (<http://www.fil.ion.ucl.ac.uk/spm/>) and NIT (<http://www.neuro.uestc.edu.cn/NIT.html>) toolboxes. The first five volumes were discarded from all fMRI scans for the magnetization equilibrium. Slice timing correction and spatially realign was performed for the remaining data. The individual T1 images were co-registered to the functional images, and segmented and normalized to the Montreal Neurologic Institute (MNI) space. Based on T1 transformation matrix, functional images were spatially normalized, resampled to  $3 \times 3 \times 3 \text{ mm}^3$  voxels, and then followed by the spatially smooth using a 6 mm full-width half maximum Gaussian kernel. Nuisance signals (six motion parameters, linear drift signal, as well as mean white matter and cerebrospinal fluid signals) were regressed out for the fMRI data. Group comparison was performed for the individual mean frame-wise

displacement (FD) calculated by averaging the relative displacement from every time point for each subject,<sup>51</sup> and no difference was found between the groups. Finally, band-pass temporal filtering (0.01–0.1 Hz) was performed.

EEG data were preprocessed using Curry 7 software (Compumedics Neuroscan) for the correction of MR gradient artifacts via template-subtraction.<sup>52</sup> The artifact template was created from a baseline-corrected sliding average of 13 consecutive volumes. Since the triggers have been delivered from the MR scanner every time an image was acquired, the template was then subtracted from the EEG segment time-locked to each volume acquisition. Next, the data were bandpass filtered (1–30 Hz) and down-sampled to 250 Hz.

The ballistocardiogram (BCG) artifacts were removed using the optimal basis set (OBS) based correction method.<sup>53</sup> QRS identification was first performed according to electrocardiograph (ECG) channel. BCG artifact occurrences associated with QRS complexes were aligned in a matrix for each EEG channel, and the temporal principal component (PCA) analysis was performed. The first three components were taken as an OBS for describing the possible shapes, amplitudes, and scales of the artifact. Then the OBS was fitted to and subtracted from each artifact occurrence.

At last, independent component analysis (ICA) was applied to manually reject the residual artifacts, especially the movement-related artifacts. Each component was characterized by a time course, and by an associated topography, which were both visually inspected for the identification and consequent rejection of artifact-related components. The rejection procedure is challenging,<sup>54</sup> because unpredictable and frustrating artifacts can be induced by movements in magnetic field. Here, the movement-related artifacts were checked referring to the FD metric generated from fMRI preprocessing. Thus, the corrected EEG were obtained by the back-projection of all the remaining independent components.

After the data were segmented as successive 2s epochs according to fMRI volume acquisition, the time points with obvious head motion in each window were visually examined and excluded for further analysis. Then, the preprocessed EEG were re-referenced to the neutral infinite reference using Reference electrode standardization technique

(REST).<sup>55</sup> For ease of calculation and avoiding the bad channel effect, 19 channels approximating the standard electrode locations in the 10–20 system were selected for the following network calculation (FP1, FP2, F3, F4, C3, C4, P3, P4, O1, O2, F7, F8, T7, T8, P7, P8, Fz, Pz, Cz).

#### 2.4. Dynamic network construction between EEG electrodes

Dynamic EEG networks were constructed using the ADTF between electrodes, which has been previously used in cognitive and epilepsy studies.<sup>56,57</sup> ADTF provided a kind of time-varying, multivariate and frequency-resolved measure, which may constitute a refinement of the dynamics of brain activity. Moreover, the variation of ADTF values within temporal epochs (2s) represented inherent dynamic spatiotemporal characteristics of epileptic activity, and showed good performance predicting epilepsy-related fluctuations.<sup>58</sup>

ADTF adopts multivariate autoregressive model (MVAR), representing the multivariate dataset  $X(t)$  as a linear combination of his own past plus additional uncorrelated white noise:

$$X(t) = \sum_{i=1}^p A(i, t)X(t-i) + E(t). \quad (1)$$

$A(i, t)$  are the matrices of dynamic model coefficients established by the Kalman filter algorithm,<sup>59</sup> and  $p$  is the model order which is chosen by the Schwarz Bayesian Criterion.<sup>60</sup> The recursive least squares (RLS) algorithm is used to solve the observation and state equations with forgetting factor.<sup>61</sup> Then, the DTF function,  $H(f)$ , can be obtained from the MVAR model by transforming Eq. (1) into the frequency domain:

$$A(f)X(f) = E(f)$$

$$\text{where } A(f) = \sum_{k=0}^p A_k e^{-j2\pi ftk} \quad (2)$$

$$X(f) = A^{-1}(f)E(f) = H(f)E(f). \quad (3)$$

The directional causal interaction from the  $j$ th to the  $i$ th node at frequency  $f$ , i.e.  $H_{ij}(f)$ , constitutes the element of the transfer matrix. Generally, integrated ADTF is defined by summing the ADTF values over

the frequency bands after normalization. Thus, the information flow of each electrode of scalp network is generated:

$$\gamma_{ij}^2(f, t) = \frac{|H_{ij}(f, t)|^2}{\sum_{m=1}^n |H_{im}(f, t)|^2}, \quad (4)$$

$$\Theta_{ij}^2(t) = \frac{\sum_{k=f_1}^{f_2} \gamma_{ij}^2(k, t)}{f_2 - f_1}. \quad (5)$$

Here,  $[f_1, f_2]$  is the frequency interval. In this study, we focused on the low frequency band, i.e. theta band (4–7 Hz), alpha band (8–12 Hz), and beta band (13–20 Hz). The mean ADTF matrix denoting the network connectivity between EEG electrodes within theta, alpha, and beta frequency band was generated respectively. Then, we calculated the variation of network connectivity in each 2s time window (one fMRI volume acquisition with  $M$  time points). The summing variation of the whole nodes, i.e.  $F_v$ , (here  $N$  is 19 electrodes across the head) was then z-scored and taken as the EEG network dynamic series in the modulation analysis.

$$F_v = \sum_{i=1}^N \sum_{j=1}^N \frac{\sum_{t=1}^M (\Theta_{ij}^2(t) - \Theta_{ij}^2(t-1)^2)}{M-1}. \quad (6)$$

#### 2.5. Thalamocortical functional couplings modulated by EEG network

In fMRI data processing, three frontal-related intrinsic networks were identified according to the previous whole-brain network segmentation based on the 1000 healthy participants sample,<sup>62</sup> including SMN, FPN, and DMN. Cortical regions of interest (ROIs) within each network were defined according to the Power's meta-analysis.<sup>63</sup>

To investigate how different thalamic circuits were modulated by the rhythmic feature, we used eight thalamus sets of Human Brainnetome Atlas<sup>64</sup> in this study. These thalamus sets can be described according to the anatomical and functional connective architecture (Supplementary material, Figure S1), including Set1: medial pre-frontal thalamus; Set2: pre-motor thalamus; Set3: sensory thalamus; Set4: rostral temporal thalamus; Set5: posterior parietal thalamus; Set6: occipital thalamus; Set7: caudal temporal thalamus; Set8: lateral pre-frontal thalamus. Next, we computed the mean signals within the cortical ROIs and thalamus

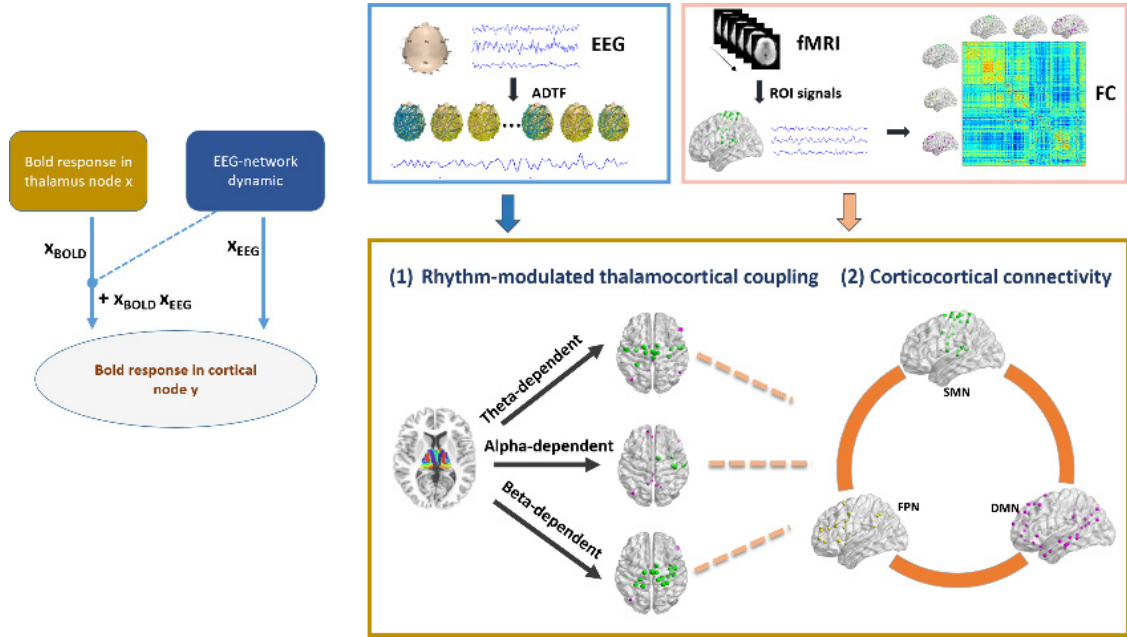


Fig. 1. Overview of the proposed thalamocortical coupling analysis modulated by rhythmic EEG network. The left sub-figure is the concept of the modulation analysis: the contribution of thalamus node  $x$  to cortical node  $y$  is modulated by EEG network metrics. The right sub-figure is the diagram of the whole study. First, rhythmic dynamic network is constructed, and fMRI signals of ROIs are extracted. Then, modulation analysis is performed between thalamocortical coupling and EEG rhythmic network. Last, the modulation effect is associated with the corticocortical functional connectivity.

Notes: ADTF: adapted directed transfer function; ROI: region of interest; FC: functional connectivity; SMN: sensorimotor network; DMN: default mode network; FPN: frontoparietal network.

sets, respectively. Then, the rhythmic EEG network-dependent functional couplings between thalamus sets and cortical regions, were examined based on the extended PPI linear model.<sup>48</sup> The PPI model was as follows:

$$y_{cortical} = \beta_0 + \beta_1 \cdot x_{thalamus} + \beta_2 \cdot x_{EEG} + \beta_3 \cdot (x_{thalamus} \cdot x_{EEG}) + \varepsilon. \quad (7)$$

Here,  $x_{thalamus}$  is the BOLD signals of one thalamus set, and  $y_{cortical}$  is the BOLD signals from cortical regions.  $x_{EEG}$  is the EEG induced signals generated by convolving the rhythm-network dynamic series with the canonical HRF, involving theta, alpha, and beta frequency band, respectively. The modulatory interaction term was the point-by-point multiplication between the BOLD signal in thalamus set and the EEG rhythm induced signals. Thus,  $\beta_3$  was the modulation contribution of rhythmic EEG to the thalamo-frontal coupling. Then, group-level statistical analyses were performed for the rhythm-dependent thalamocortical functional

couplings. The whole framework was illustrated in Fig. 1.

## 2.6. Association between thalamocortical coupling and corticocortical connectivity

To examine the association between rhythm-dependent thalamocortical coupling and corticocortical network, we analyzed the correlations between the rhythmic modulatory effect ( $\beta_3$ ) and functional connectivity (FC) between cortical regions. Corticocortical FC was obtained according to the Pearson correlation of BOLD signals between cortical ROIs among the three intrinsic networks, i.e. SMN, FPN, and DMN. The modulatory thalamocortical effect for one network and inter-cortical FC between this network and others was associated based on distance correlation.<sup>65</sup>

Distance correlation is a general measure of dependence of two multivariate datasets  $X, Y$ . The first step is to compute the Euclidean distance in

node-space between each pair of variates for  $X$  and  $Y$  separately:

$$\begin{aligned} a_{i,j} &= \sqrt{\sum_{k=1}^{v_1} (X_{ik} - X_{jk})^2} \quad i, j = 1, \dots, n \\ b_{i,j} &= \sqrt{\sum_{k=1}^{v_2} (Y_{ik} - Y_{jk})^2} \quad i, j = 1, \dots, n. \end{aligned} \quad (8)$$

Here,  $X$  is the modulatory effect from thalamus sets to cortical nodes in one given intrinsic network (e.g. SMN, FPN, DMN), that is, the row consisted of  $n$  cortical nodes in the network and the column was the thalamus sets ( $v_1$ );  $Y$  is the FC matrices, that is, the row denoted  $n$  cortical nodes of the given network and the column is the connected nodes ( $v_2$ ) in another network. Then, U-centering was applied to the acquired Euclidean distance to ensure the correlation estimates were not biased by the number of nodes.

$$A_{i,j} = \begin{cases} a_{ij} \frac{1}{n-2} \sum_{l=1}^n a_{i,l} \frac{1}{n-2} \sum_{k=1}^n a_{k,j} \\ \quad + \frac{1}{(n-1)(n-2)} \sum_{k,l=1}^n a_{k,l}, & i \neq j \\ 0, & i = j \end{cases} \quad (9)$$

Therefore, the distance correlation can be computed using the distance covariance and distance variance based on the U-centering matrix.

$$dCor(X, Y) = \begin{cases} \sqrt{\frac{dCov(X, Y)}{\sqrt{dVar(X)dVar(Y)}}} & dCov(X, Y) > 0 \\ 0 & dCov(X, Y) \leq 0 \end{cases}$$

$$dCov(X, Y) = \frac{1}{K} \sum_{i,j=1}^n A_{i,j} B_{i,j}; \quad (10)$$

$$dVar(X) = \frac{1}{K} \sum_{i,j=1}^n A_{i,j}^2;$$

$$dVar(Y) = \frac{1}{K} \sum_{i,j=1}^n B_{i,j}^2;$$

## 2.7. Statistical methods

Group-level statistical tests were conducted for rhythm-dependent thalamocortical couplings. Before the statistical tests, the normality of the data distribution was first examined based on the two-sided goodness-of-fit Lilliefors test. Then one sample  $t$ -test was performed for each group, and the statistic threshold was set to  $P < 0.05$  without correction. Moreover, two-sample  $t$ -test ( $P < 0.05$ ) between groups was performed for the mean effects of the nodes within intrinsic networks, where the nodes were selected using the union of nodes with statistical significance in the one sample  $t$ -test of the three groups. In addition, for the relationship between rhythm-dependent thalamocortical coupling and corticocortical network, the data distribution was also tested. Then, two sample  $t$ -test ( $P < 0.05$ ) between groups was conducted for the correlation values. In between-group comparisons, age and gender were regressed out as the covariates.

## 3. Results

### 3.1. Thalamocortical functional coupling modulated by rhythmic EEG network

Averaged EEG network variation across time points was first compared between groups, and epilepsy groups showed larger network variations than HC for all frequency bands ( $P < 0.01$ , two-sample  $t$ -test). No significant difference was observed between JME and FLE group. Thalamocortical couplings modulated by rhythmic network were then analyzed. Significant rhythm-dependent modulation was demonstrated (Fig. S2). Moreover, the modulatory effects were also influenced by thalamus sets. Generally, thalamus Set6, Set7 were more sensitive regions which were involved in rhythmic modulation in healthy group for all frequency bands.

For theta, obvious positive modulatory couplings were represented between thalamus Set6, Set7 and SMN in HC group. Whereas in JME and FLE, these positive modulatory interactions were significantly decreased. In addition, slight modulatory couplings were also found between thalamus sets and DMN, as well as FPN. Reduced thalamus-FPN couplings were found in FLE. Figure 2 illustrated the one sample  $t$ -test results and between-group

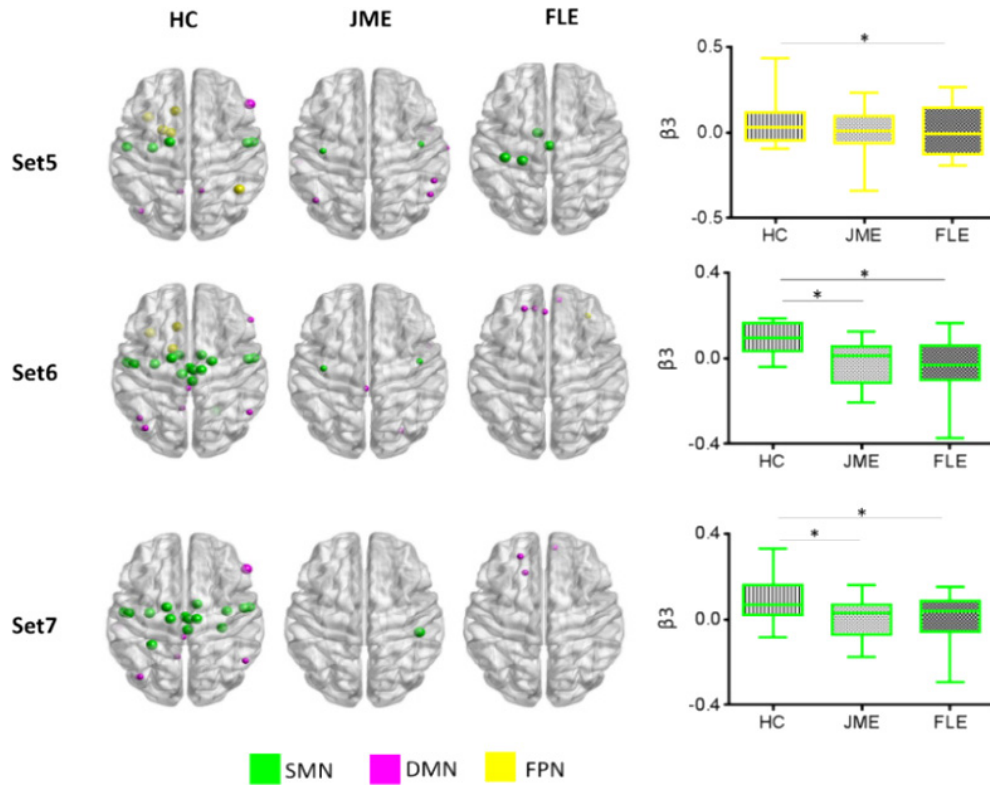


Fig. 2. (Color online) The thalamocortical couplings modulated by theta frequency band. Left: The dots on the brain template were cortical regions with significant theta-dependent thalamocortical coupling for each group (one-sample  $t$ -test,  $P < 0.05$ ). Different color of the dots represented different cortical networks. Dots of larger size denoted positive modulation and dots of smaller size denoted negative modulation. Right: The results of group comparisons with significant difference (two-sample  $t$ -test,  $P < 0.05$ ). Similarly, the color of the boxplots was corresponding to different cortical networks. Decreased thalamus-SMN modulatory couplings were found both in JME and FLE, while reduced thalamus-FPN couplings were found in FLE.

Note: SMN: sensorimotor network; DMN: default mode network; FPN: frontoparietal network; Set5: posterior parietal thalamus; Set6: occipital thalamus; Set8: lateral pre-frontal thalamus.

comparison with statistical significance. Different colors in the group-level modulation distribution and the between-group comparison results denoted different cortical networks. No significant difference was found between JME and FLE.

Alpha-dependent modulatory couplings were shown in Fig. 3. Most thalamus sets demonstrated negative modulatory couplings to DMN in HC group. Nevertheless, abnormal alpha-dependent modulatory effect was distinctively found in JME. The negative modulatory couplings from thalamus to DMN were changed and tended to be positive. Furthermore, JME showed increased modulatory couplings between thalamus and SMN, which was not found in FLE group. For beta frequency, positive modulatory couplings between thalamus sets and SMN were still

dominant in HC group. However, distinct increased couplings from thalamus to FPN were represented in FLE (Fig. 4).

In addition, supplementary analyses were conducted, and the functional couplings between thalamus and 258 cortical ROIs (atlas from Power's meta-analysis) of the whole brain<sup>63</sup> was computed (Figs. S3–S5). Here, 7 networks were included: the visual network (VN), SMN, dorsal attention network (DAN), ventral attention network (VAN), limbic network (LN), frontoparietal network (FPN), and DMN. The group-level comparison results were demonstrated in Supplemental Materials (Figs. S6–S8). The results showed that the VN and LN were two another vulnerable networks in both JME and FLE patients.

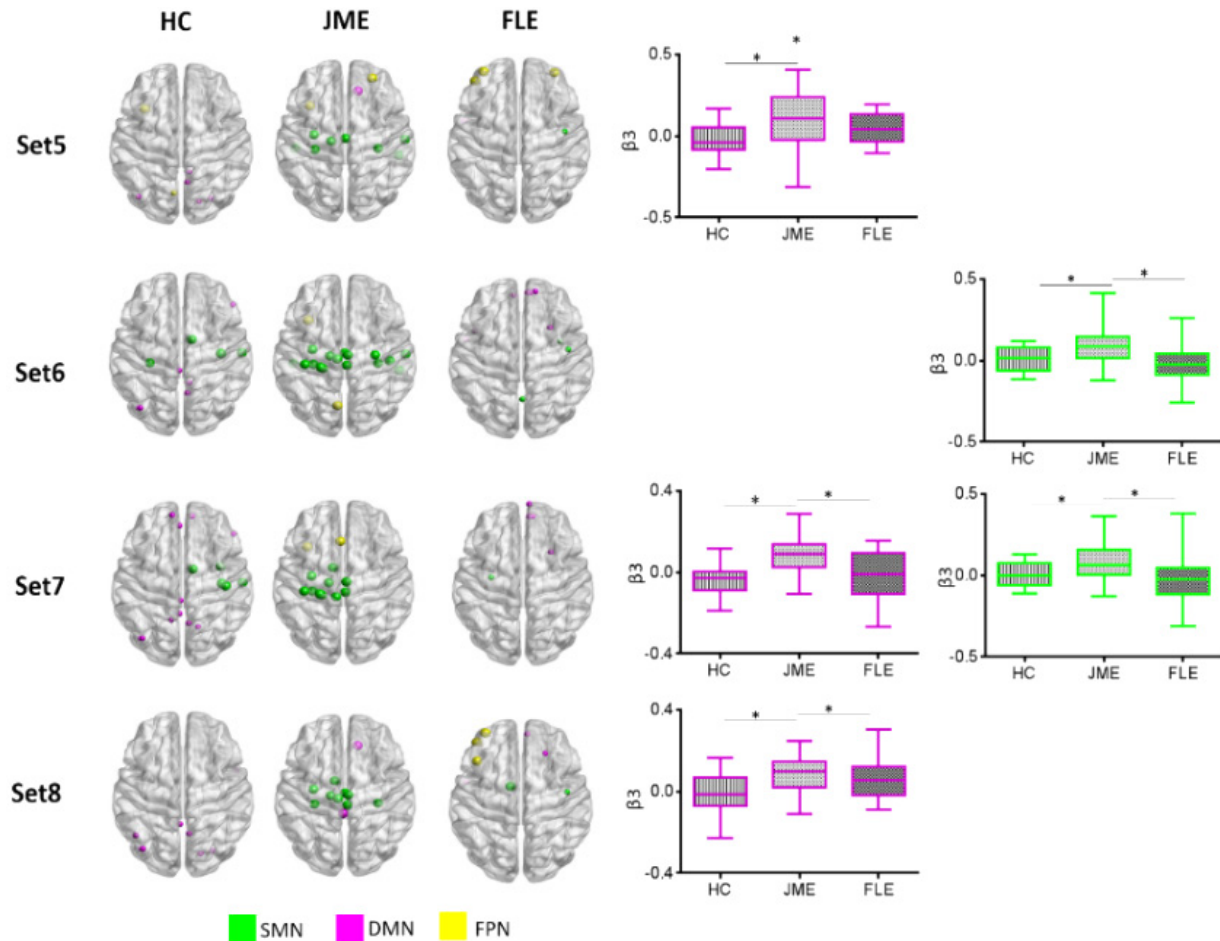


Fig. 3. The thalamocortical couplings modulated by alpha frequency band. Left: The dots on the brain template were cortical regions with significant alpha-dependent thalamocortical coupling for each group (one-sample  $t$ -test,  $P < 0.05$ ). Different color of the dots represented different cortical networks. Dots of larger size denoted positive modulation and dots of smaller size denoted negative modulation. Right: The results of group comparisons with significant difference (two-sample  $t$ -test,  $P < 0.05$ ). Similarly, the color of the boxplots was corresponding to different cortical networks. JME showed increased modulatory effect in thalamus-SMN and thalamus-DMN couplings, while in the FLE, this effect was not significant.

Notes: SMN: sensorimotor network; DMN: default mode network; FPN: frontoparietal network; Set5: posterior parietal thalamus; Set6: occipital thalamus; Set7: caudal temporal thalamus; Set8: lateral pre-frontal thalamus.

### 3.2. Altered association between thalamocortical coupling and corticocortical connectivity in epilepsy

Altered association between corticocortical connectivity and thalamocortical coupling was found in epilepsy group. The results were showed in Fig. 5(A). Comparing to HC, alpha-modulated thalamus-SMN couplings in JME demonstrated increased correlation with SMN-related connectivity, i.e. SMN-FPN and SMN-DMN connectivity. While in FLE group, decreased correlation was found between

theta-modulated thalamus-FPN couplings and FPN-related pathway, including FPN-SMN and FPN-DMN connectivity.

### 3.3. Correlation of thalamocortical/corticocortical and clinical features

Pearson correlations between the duration of epilepsy and thalamocortical coupling, as well as the corticocortical connectivity, were conducted. It was observed that increased alpha-modulated thalamus-SMN couplings were associated with the longer

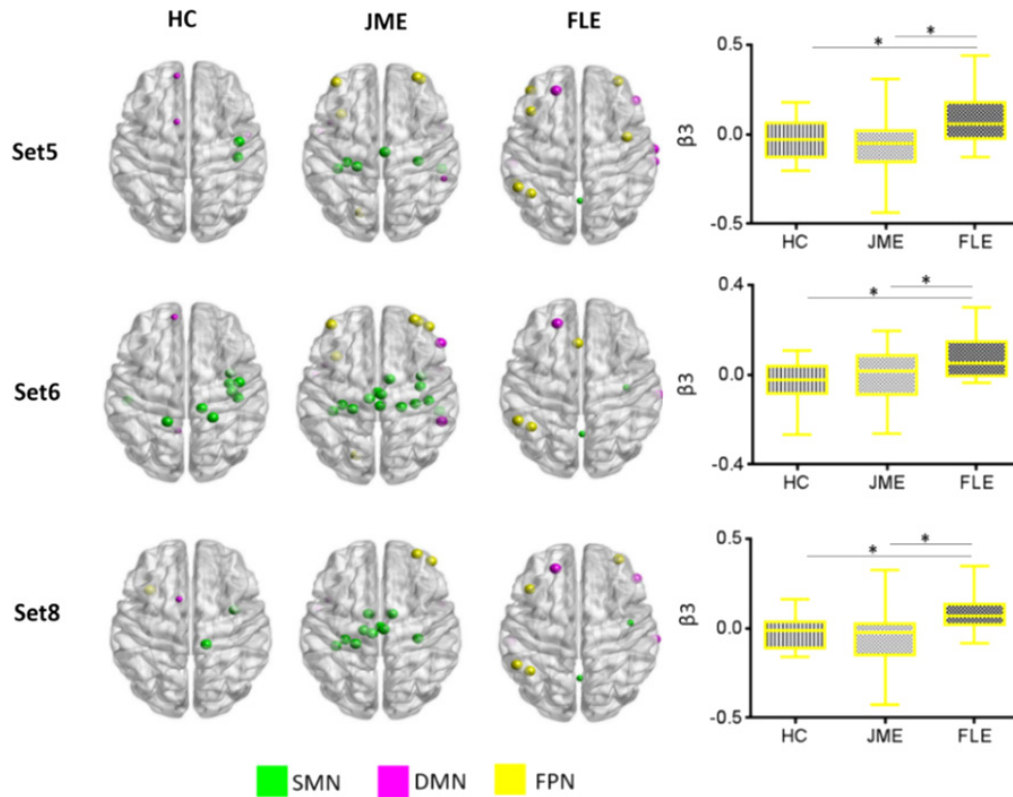


Fig. 4. The thalamocortical coupling modulated by beta frequency band. Left: The dots on the brain template were cortical regions with significant beta-dependent thalamocortical coupling for each group (one-sample  $t$ -test,  $P < 0.05$ ). Different color of the dots represented different cortical networks. Dots of larger size denoted positive modulation and dots of smaller size denoted negative modulation. Right: The results of group comparisons with significant difference (two-sample  $t$ -test,  $P < 0.05$ ). Similarly, the color of the boxplots was corresponding to different cortical networks. Distinct increased thalamus-FPN couplings were represented in FLE.

Notes: SMN: sensorimotor network; DMN: default mode network; FPN: frontoparietal network; Set5: posterior parietal thalamus; Set6: occipital thalamus; Set8: lateral pre-frontal thalamus.

epilepsy duration in JME [Fig. 5(B)]. Moreover, thalamus Set6 and Set7 were involved in this correlation.

#### 4. Discussion

In this study, we tested the hypothesis that the thalamocortical functional couplings were modulated by rhythmic EEG network features. Increased thalamus-SMN couplings in JME were strongly modulated by alpha band, and this modulation pattern had enhanced association with SMN-related inter-cortical connectivity (SMN-DMN and SMN-FPN connectivity). On the contrary, decreased theta-dependent thalamus-FPN couplings were found in FLE, and the association between the modulatory coupling pattern and inter-cortical connectivity

with DMN and SMN was also reduced. For the modulation by beta band, increased thalamus-FPN couplings were only found in FLE compared to HC and JME. These findings may contribute to understanding the potential disease-related representation in JME and FLE group.

Previous studies have reviewed that thalamocortical circuit can generate different types of cortical oscillation and facilitate the communication between brain regions.<sup>4,66</sup> Some research has used computational models and animal vitro-recording to examine the cortico-thalamic feedback with the modulation of cortical synchronous oscillation, particularly to explore the genesis of epilepsy seizures.<sup>2,67</sup> Neural oscillation based on EEG has been frequently detected to uncover the potential pathophysiology in

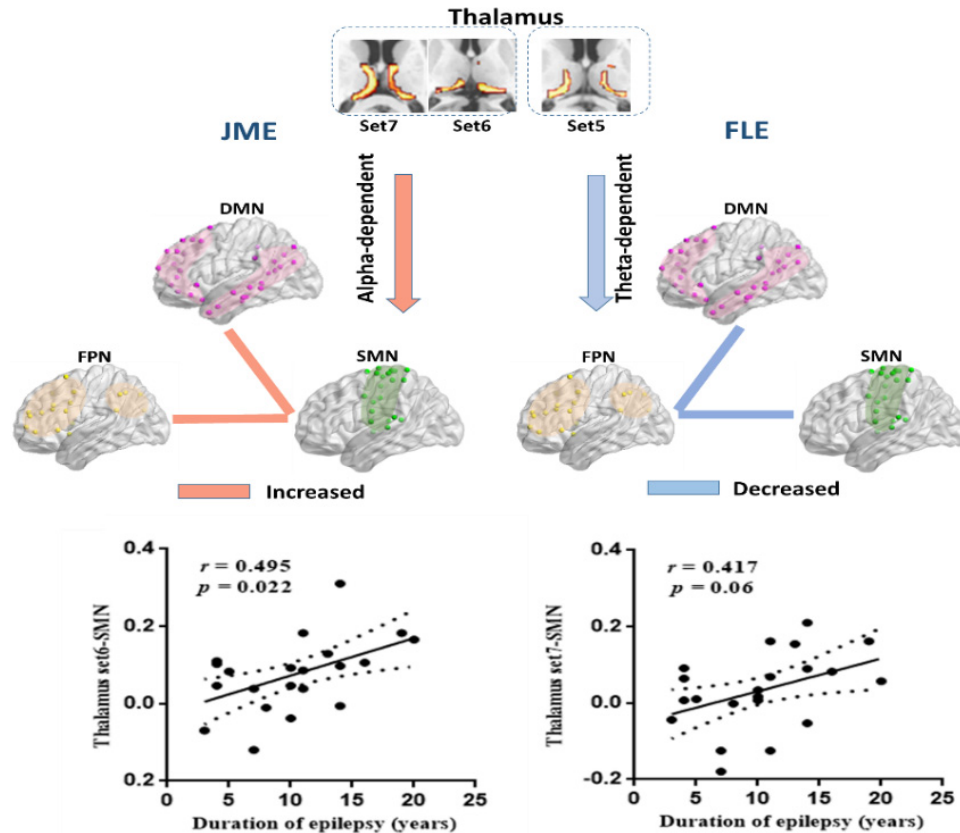


Fig. 5. (Color online) The top: The altered association between EEG network-dependent thalamocortical coupling and corticocortical inter-network connectivity in JME and FLE. The red and blue lines denoted increased correlations and decreased correlations ( $P < 0.05$ ). In JME, alpha-modulated thalamus–SMN couplings showed increased association with SMN–FPN connectivity and SMN–DMN connectivity. While in FLE, decreased correlation was found between theta-modulated thalamus–FPN couplings and FPN-related pathway, including FPN–SMN and FPN–DMN connectivity. The bottom: Alpha-dependent thalamus–SMN coupling was positively correlated with the epilepsy duration in JME.

neurologic disorders.<sup>68–72</sup> Here, scalp rhythmic networks were constructed using ADTF. The estimation of ADTF was suggested insensitive to volume conduction which describes the propagation of the electromagnetic field without phase difference.<sup>73</sup> This paper applied EEG–fMRI fusion model to detect what the cortical network organization may serve in thalamocortical circuit, and built links between thalamocortical mis-coupling and rhythmic oscillation in epilepsy. In HC group, the results represented strong negative alpha modulation effect contributing to thalamus–DMN couplings. Previous studies have revealed that alpha rhythm was strongly associated with DMN,<sup>74</sup> and had the specific negative effect to thalamus–DMN connectivity.<sup>75</sup> The consistent negative modulation in the current study may be associated with the inhibition coordination of alpha to the thalamocortical connectivity. For theta and beta

frequency bands in HC, positive modulation effects mainly acted on thalamus–SMN couplings, representing the dependence between the rhythm and certain thalamic projections, and thus facilitating the inter-region communication in thalamocortical and corticocortical circuit. Moreover, it was shown that the parietal, occipital, and temporal thalamus was predominately involved in the thalamocortical modulation, implying the complex thalamocortical spatial pattern depending on the dynamic cortical network feedback.

In epilepsy group, altered modulatory thalamocortical couplings were represented. As theta band (3–7 Hz) was much more vulnerable due to the epileptic discharges, the disturbed theta-dependent thalamus–SMN, thalamus–FPN, as well as the thalamus–LN couplings (Fig. S6) in epilepsy group were interpretable and may imply the

pathophysiological factors associated with the worse performance of motor coordination and executive functions in IGE and focal epilepsy patients.<sup>76,77</sup> Besides, distinct representations were found resulting from the interactions between thalamo-frontal coupling and rhythmic network in JME and FLE. Notably, the enhancement of thalamocortical coupling in JME was strongly associated with alpha band. Hyperconnectivity and hyperexcitability in motor system and in thalamus-SMN connectivity has been widely observed in JME.<sup>78,79</sup> Although the alpha-modulation effect on SMN was not sensitive in HC, the increased positive effects in JME may suggest the altered alpha oscillation regulation on thalamus-SMN couplings because of the impairment and hyperexcitability near SMN.<sup>80</sup> Moreover, JME was characterized by a frontocentral predominance of ictal EEG, and the altered modulatory couplings may aggravate the inter-cortical interaction related with SMN, including SMN-DMN and SMN-FPN connectivity. Therefore, SMN was assumed to be a crucial node linking subcortical and cortical regions in JME, and furthermore facilitating the generalized epileptic activity across the whole brain. The correlation with epilepsy duration further implied that the abnormal couplings linking posterior and medial nucleus of thalamus with SMN regions in this study may be important biomarker of severity of the disease.<sup>81,82</sup> In addition, it was interesting that enhanced positive alpha-modulated thalamus-DMN couplings was found in JME. A lot of evidence has emerged indicating the disturbance of the DMN in epilepsy.<sup>34,83</sup> The suspension of BOLD response in DMN was found related to the epileptic discharges.<sup>36,84</sup> One previous study also demonstrated decreased connectivity between thalamus and precuneus.<sup>78</sup> In fact, the conversed positive modulation in this study may elucidate one kind of regulation of alpha rhythm in JME. Moreover, thalamus and the posterior areas were key regions relating to the generation of alpha oscillation.<sup>85</sup> The increased association between the abnormal thalamus-DMN connectivity and alpha rhythm may have implications for understanding the neuropathology in epileptic brain. In addition, enhanced thalamus-VN couplings were also found in both JME and FLE with alpha modulation (Fig. S7), which suggested the association of the visual pathway impairment with alpha dynamic in epilepsy patients.<sup>86</sup>

FLE was frequently characterized by the complex functional organization of the frontal lobe and its reciprocal connections with other cortical, subcortical areas,<sup>87</sup> which lead to various impairments in cognitive functioning and behavioral disorders. Previous network analysis also demonstrated that abnormality in FLE patients was highly related to FPN system,<sup>88</sup> and FPN has long been implicated mediating the top-down control and supporting goal-directed cognition.<sup>89</sup> In this study, altered thalamus-FPN coupling with beta modulation was only found in FLE. As beta rhythm played a key role in top-down (frontoparietal) processing,<sup>90</sup> the abnormal modulation may provide interpretations for the vigorous frontoparietal activity and executive deficit in FLE.<sup>34,91</sup> In addition, decreased association between thalamus-FPN couplings and corticocortical connectivity due to the theta-mediated mechanism was found in FLE. The reduced theta-modulation on the couplings between posterior medial thalamus and FPN may be attributed to the interruption of the epileptic discharges, and consequently cause the alteration in FPN related pathway (FPN-SMN and FPN-DMN). Therefore, it was suggested that FPN would have a potential role as circuit biomarkers for the pathophysiology and intervention process in FLE.

This study provided a new approach to link the spatial thalamocortical circuit with the rhythmic organization resulting from the synchronization of neural ensembles. Cortical spatiotemporal organization can be specifically exhibited by scalp EEG,<sup>6,7</sup> which also enables to uncover the potential pathophysiology in neurologic disorders.<sup>92,93</sup> The rhythm-dependent thalamocortical coupling in this study demonstrated the associations between the rhythm and thalamic projections, which may facilitate the homeostasis in brain in terms of the subcortical-cortical communications. Comparing to HC, much larger EEG network variation in epilepsy group was found for all frequency bands. As this study was performed interictal, we tend to consider that the altered EEG network and the thalamocortical uncoupling was resulting from the cumulative effect in epileptic and medicated brain suffering from the long-term epileptic activity.

However, there are several methodological considerations and limitations in this study. The first concern is the lack of the direct association with

the paroxysmic epileptic activity. As the study was performed interictal, the modulatory thalamocortical uncoupling in epilepsy group was supposed to reflect the cumulative effect in epileptic brain suffering from long-term epileptic activity. Another limitation is the brain atlas used in this study. Different atlas stemming from distinct parcellation framework may influence the connectivity between regions from the atlas. However, when one alternative atlas (Human Brainnetome Atlas including 230 cortical areas) was used in this study, most consistent results were observed. Third, we used global rhythmic network variation property between EEG electrodes to calculate the modulatory thalamocortical coupling. The rhythmic activities, i.e. theta, alpha, beta, always have certain spatial distribution, therefore, rhythmic activity from local and more delicate spatial distribution may increase the significance of modulation effect. Moreover, as the rhythmic network was obtained using ADTF with 19 electrodes, a high electrode density (64 channels) can be carried out in the future work and more informative results may be drawn. Next, the effect from medication was not taken into consideration because of the diversity of medications and the distinct mechanisms of these drugs, which may affect the result of between-group comparisons. Finally, due to the limited sample size, future studies should include larger sample sizes to determine the pathophysiological mechanisms underlying the altered interaction between EEG rhythm and thalamocortical network in epilepsy.

## 5. Conclusion

In conclusion, this study provided a novel method to investigate the modulatory interactions between the thalamocortical connectivity and EEG rhythmic network dynamics. The results showed frequency-dependent characteristics of these modulations. Distinct aberrant thalamocortical couplings were showed in JME and FLE patients. Associations between thalamocortical couplings and corticocortical connectivity due to the rhythm-mediated mechanism was also investigated. The specificity of modulation with different rhythm would imply that SMN played a crucial role linking subcortical and cortical regions in JME; however, the FPN was important joinpoint in the subcortical-cortical circuit in FLE. This modulation analysis may have implications for

understanding and intervention of the aberrant thalamocortical circuit in generalized and focal epilepsy.

## Authors and Contributors

Conceived and designed the work: YQ, SJ, XZ. Acquired the data: LD, JL, XZ, NZ, YC. Analyzed the data: YQ, NZ. Wrote the paper: YQ, TZ, CL. All authors revised the work for important intellectual content. All of the authors have read and approved the manuscript.

## Acknowledgments

This work was partly supported by the grant from National Key R&D Program of China (2018YFA0701400), the grants from the National Nature Science Foundation of China (grant number: 61933003, 81701778, 81771822, 81861128001, U1833130, and 31771149), the Project of Science and Technology Department of Sichuan Province (2016HH0005 and 2019YJ0179) and the CAMS Innovation Fund for Medical Sciences(CIFMS) (No.2019-12M-5-039).

## Note Added

This study is our original unpublished work and the manuscript or any variation of it has not been submitted to another publication previously.

## Conflict of interest

None of the authors has any conflict of interest to disclose.

## References

1. B. J. Baars, S. Franklin and T. Z. Ramsay, Global workspace dynamics: Cortical “binding and propagation” enables conscious contents, *Front. Psychol* **4** (2013) 200:1–22.
2. T. Bal, D. Debay and A. Destexhe, Cortical feedback controls the frequency and synchrony of oscillations in the visual thalamus, *J. Neurosci.* **20** (2000) 7478–7488.
3. U. Ribary, Dynamics of thalamo-cortical network oscillations and human perception, *Prog. Brain Res.* **150** (2005) 127–142.
4. Y. B. Saalmann, Intralaminar and medial thalamic influence on cortical synchrony, information transmission and cognition, *Front. Syst. Neurosci.* **8** (2014) 83.

5. D. C. Van Essen, Corticocortical and thalamocortical information flow in the primate visual system, *Cort. Funct.* **149** (2005) 173–185.
6. E. R. John, From synchronous neuronal discharges to subjective awareness?, **150** (2005) 143–593.
7. M. A. L. Nicolelis, L. A. Baccala, R. C. S. Lin and J. K. Chapin, Sensorimotor encoding by synchronous neural ensemble activity at multiple levels of the somatosensory system, *Science* **268** (1995) 1353–1358.
8. W. Singer, Neuronal synchrony: A versatile code for the definition of relations?, *Neuron* **24** (1999) 49–65.
9. M. N. Shadlen and J. A. Movshon, Synchrony unbound: A critical evaluation of the temporal binding hypothesis, *Neuron* **24** (1999) 67–77.
10. M. Ahmadlou, H. Adeli and A. Adeli, Spatiotemporal analysis of relative convergence of EEGs reveals differences between brain dynamics of depressive women and men, *Clin. EEG Neurosci.* **44** (2013) 175–181.
11. J. delEtoile and H. Adeli, Graph theory and brain connectivity in Alzheimer’s disease, *Neuroscientist* **23** (2017) 616–626.
12. M. Ahmadlou, H. Adeli and A. Adeli, Fuzzy synchronization likelihood-wavelet methodology for diagnosis of autism spectrum disorder,” *J. Neurosci. Methods* **211** (2012) 203–209.
13. M. Ahmadlou, A. Adeli, R. Bajo and H. Adeli, Complexity of functional connectivity networks in mild cognitive impairment subjects during a working memory task, *Clin. Neurophysiol.* **125** (2014) 694–702.
14. Y. Jiang, C. Luo, X. Li, M. Duan, H. He, X. Chen, H. Yang, J. Gong, X. Chang, M. Woelfer, B. B. Biswal and D. Yao, Progressive reduction in gray matter in patients with schizophrenia assessed with MR imaging by using causal network analysis, *Radiology* **287** (2018) 633–642.
15. A. Jahangiri and D. M. Durand, Phase resetting analysis of high potassium spiking epileptiform activity in CA3 region of the rat hippocampus, *Int. J. Neural Syst.* **21** (2011) 127–138.
16. G. P. Ren, J. Q. Yan, Z. X. Yu, D. Wang, X. N. Li, S. S. Mei, J. D. Dai, X. L. Li, Y. L. Li, X. F. Wang and X. F. Yang, Automated detector of high frequency oscillations in epilepsy based on maximum distributed peak points, *Int. J. Neural Syst.* **28**(2017) 1750029:1–20.
17. A. Stoller, Slowing of the alpha-rhythm of the electroencephalogram and its association with mental deterioration and epilepsy, *J. Mental Sci.* **95** (1949) 972–984.
18. D. Sherman, N. Zhang, S. Garg, N. V. Thakor, M. A. Mirski, M. A. White and M. J. Hinich, Detection of nonlinear interactions of EEG alpha waves in the brain by a new coherence measure and its application to epilepsy and anti-epileptic drug therapy, *Int. J. Neural Syst.* **21** (2011) 115–126.
19. P. A. Valdes-Hernandez, A. Ojeda-Gonzalez, E. Martinez-Montes, A. Lage-Castellanos, T. Virues-Alba, L. Valdes-Urrutia and P. A. Valdes-Sosa, White matter architecture rather than cortical surface area correlates with the EEG alpha rhythm, *NeuroImage* **49** (2010) 2328–2339.
20. J. Engel, A proposed diagnostic scheme for people with epileptic seizures and with epilepsy: Report of the ILAE Task Force on Classification and Terminology, *Epilepsia* **42** (2001) 796–803.
21. C. Luo, Y. D. Zhang, W. F. Cao, Y. Huang, F. Yang, J. J. Wang, S. P. Tu, X. M. Wang and D. Z. Yao, Altered structural and functional feature of striato-cortical circuit in benign epilepsy with centrotemporal spikes, *Int. J. Neural Syst.* **25**(6) (2015) 1550027.
22. H. Adeli and S. Ghosh-Dastidar, *Automated EEG-Based Diagnosis of Neurological Disorders: Inventing the Future of Neurology* (CRC Press, 2010).
23. J. T. Paz, J. M. Deniau and S. Charpier, Rhythmic bursting in the cortico-subthalamo-pallidal network during spontaneous genetically determined spike and wave discharges, *J. Neurosci.* **25** (2005) 2092–2101.
24. M. Guye, J. Regis, M. Tamura, F. Wendling, A. M. Gonigal, P. Chauvel and F. Bartolomei, The role of corticothalamic coupling in human temporal lobe epilepsy, *Brain* **129** (2006) 1917–1928.
25. C. Vollmar, J. O’Muircheartaigh, G. J. Barker, M. R. Symms, P. Thompson, V. Kumari, J. S. Duncan, D. Janz, M. P. Richardson and M. J. Koepp, Motor system hyperconnectivity in juvenile myoclonic epilepsy: A cognitive functional magnetic resonance imaging study, *Brain* **134** (2011) 1710–1719.
26. S. Ghosh-Dastidar and H. Adeli, Improved spiking neural networks for EEG classification and epilepsy and seizure detection, *Integr. Comput-Aid E* **14** (2007) 187–212.
27. K. T. Tapani, S. Vanhatalo and N. J. Stevenson, Time-varying EEG correlations improve automated neonatal seizure detection,” *Int. J. Neural Syst.* **29**(4) (2019) 1850030.
28. C. Koutlis, V. K. Kimiskidis and D. Kugiumtzis, Identification of hidden sources by estimating instantaneous causality in high-dimensional biomedical time series, *Int. J. Neural Syst.* **29** (2019).
29. S. Ghosh-Dastidar and H. Adeli, A new supervised learning algorithm for multiple spiking neural networks with application in epilepsy and seizure detection, *Neural Netw.* **22** (2009) 1419–1431.
30. M. Ahmadlou and H. Adeli, Functional community analysis of brain: A new approach for EEG-based investigation of the brain pathology, *NeuroImage* **58** (2011) 401–408.

31. D. Janz, Epilepsy with impulsive petit mal (juvenile myoclonic epilepsy), *Acta Neurol. Scand.* **72** (1985) 449–459.
32. C. P. Panayiotopoulos, T. Obeid and A. R. Tahan, Juvenile myoclonic epilepsy - a 5-year prospective study, *Epilepsia* **35** (1994) 285–296.
33. C. Lee, C. H. Im, Y. S. Koo, J. A. Lim, T. J. Kim, J. I. Byun, J. S. Sunwoo, J. Moon, D. W. Kim, S. T. Lee, K. H. Jung, K. Chu, S. K. Lee and K. Y. Jung, Altered network characteristics of spike-wave discharges in juvenile myoclonic epilepsy, *Clin. EEG Neurosci.* **48** (2017) 111–117.
34. L. Dong, H. Li, Z. He, S. Jiang, B. Klugah-Brown, L. Chen, P. Wang, S. Tan, C. Luo and D. Yao, Altered local spontaneous activity in frontal lobe epilepsy: A resting-state functional magnetic resonance imaging study, *Brain Behav.* **6** (2016) e00555.
35. F. Fahoum, R. Lopes, F. Pittau, F. F. Dubeau and J. Gotman, Widespread epileptic networks in focal epilepsies: EEG-fMRI study, *Epilepsia* **53** (2012) 1618–1627.
36. J. Gotman, C. Grova, A. Bagshaw, E. Kobayashi, Y. Aghakhani and F. Dubeau, Generalized epileptic discharges show thalamocortical activation and suspension of the default state of the brain, *Proc. Natl. Acad. Sci. USA* **102** (2005) 15236–15240.
37. D. B. Dong, M. J. Duan, Y. L. Wang, X. X. Zhang, X. Y. Jia, Y. J. Li, F. Xin, D. Z. Yao and C. Luo, Reconfiguration of dynamic functional connectivity in sensory and perceptual system in schizophrenia, *Cereb. Cortex* **29** (2019) 3577–3589.
38. H. He, C. Luo, Y. L. Luo, M. J. Duan, Q. Z. Yi, B. B. Biswal and D. Z. Yao, Reduction in gray matter of cerebellum in schizophrenia and its influence on static and dynamic connectivity, *Human Brain Mapping* **40** (2019) 517–528.
39. X. Y. Jia, Y. Xie, D. B. Dong, H. N. Pei, S. S. Jiang, S. Ma, Y. Huang, X. X. Zhang, Y. H. Wang, Q. Zhu, Y. N. Zhang, D. Z. Yao, L. Yu and C. Luo, Reconfiguration of dynamic large-scale brain network functional connectivity in generalized tonic-clonic seizures, *Human Brain Mapping* (2019) 67–79.
40. P. Fries, J. H. Reynolds, A. E. Rorie and R. Desimone, Modulation of oscillatory neuronal synchronization by selective visual attention, *Science* **291** (2001) 1560–1563.
41. D. J. Heeger and D. Ress, What does fMRI tell us about neuronal activity?, *Nat. Rev. Neurosci.* **3** (2002) 142–151.
42. J. W. Scannell and M. P. Young, Neuronal population activity and functional imaging, *Proc. R. Soc. B-Biol. Sci.* **266** (1999) 875–881.
43. F. Deligianni, M. Centeno, D. W. Carmichael and J. D. Clayden, Relating resting-state fMRI and EEG whole-brain connectomes across frequency bands, *Front. Neurosci.* **8** (2014) 258:1–16.
44. A. N. Nielsen and M. Lauritzen, Coupling and uncoupling of activity-dependent increases of neuronal activity and blood flow in rat somatosensory cortex, *J. Physiol. London* **533** (2001) 773–785.
45. P. Tewarie, M. G. Bright, A. Hillebrand, S. E. Robinson, L. E. Gascoyne, P. G. Morris, J. Meier, P. Van Mieghem and M. J. Brookes, Predicting haemodynamic networks using electrophysiology: The role of non-linear and cross-frequency interactions, *NeuroImage* **130** (2016) 273–292.
46. S. Ogawa, T. M. Lee, R. Stepnoski, W. Chen, X. H. Zhuo and K. Ugurbil, An approach to probe some neural systems interaction by functional MRI at neural time scale down to milliseconds, *Proc. Natl. Acad. Sci. USA* **97** (2000) 11026–11031.
47. X. Di, R. C. Reynolds and B. B. Biswal, "Imperfect (de)convolution may introduce spurious psychophysiological interactions and how to avoid it, *Human Brain Mapping* **38** (2017) 1723–1740.
48. K. J. Friston, C. Buechel, G. R. Fink, J. Morris, E. Rolls and R. J. Dolan, Psychophysiological and modulatory interactions in neuroimaging, *NeuroImage* **6** (1997) 218–229.
49. R. S. Fisher, J. H. Cross, J. A. French, N. Higurashi, E. Hirsch, F. E. Jansen, L. Lagae, S. L. Moshe, J. Peltola, E. Roulet Perez, I. E. Scheffer and S. M. Zuberi, Operational classification of seizure types by the International League Against Epilepsy: Position Paper of the ILAE Commission for Classification and Terminology, *Epilepsia* **58** (2017) 522–530.
50. I. E. Scheffer, S. Berkovic, G. Capovilla, M. B. Connolly, J. French, L. Guilhoto, E. Hirsch, S. Jain, G. W. Mathern, S. L. Moshe, D. R. Nordli, E. Perucca, T. Tomson, S. Wiebe, Y. H. Zhang and S. M. Zuberi, ILAE classification of the epilepsies: Position paper of the ILAE Commission for Classification and Terminology, *Epilepsia* **58** (2017) 512–521.
51. J. D. Power, K. A. Barnes, A. Z. Snyder, B. L. Schlaggar and S. E. Petersen, Spurious but systematic correlations in functional connectivity MRI networks arise from subject motion, *NeuroImage* **59** (2012) 2142–2154.
52. P. J. Allen, O. Josephs and R. Turner, A method for removing imaging artifact from continuous EEG recorded during functional MRI, *Neuroimage* **12** (2000) 230–239.
53. R. K. Niazy, C. F. Beckmann, G. D. Iannetti, J. M. Brady and S. M. Smith, Removal of fMRI environment artifacts from EEG data using optimal basis sets, *NeuroImage* **28** (2005) 720–737.
54. N. Mammone and F. C. Morabito, Enhanced automatic wavelet independent component analysis for electroencephalographic artifact removal, *Entropy-Switz* **16** (2014) 6553–6572.
55. D. Z. Yao, A method to standardize a reference of scalp EEG recordings to a point at infinity, *Physiol. Meas.* **22** (2001) 693–711.

56. P. van Mierlo, E. Carrette, H. Hallez, K. Vonck, D. Van Roost, P. Boon and S. Staelens, Accurate epileptogenic focus localization through time-variant functional connectivity analysis of intracranial electroencephalographic signals, *Neuroimage* **56** (2011) 1122–1133.
57. L. Y. Zhang, Y. Liang, F. L. Li, H. B. Sun, W. J. Peng, P. S. Du, Y. J. Si, L. M. Song, L. Yu and P. Xu, Time-varying networks of inter-ictal discharging reveal epileptogenic zone, *Front. Comput. Neurosci.* **11** (2017).
58. Y. Qin, S. Jiang, Q. Zhang, L. Dong, X. Jia, H. He, Y. Yao, H. Yang, T. Zhang, C. Luo and D. Yao, BOLD-fMRI activity informed by network variation of scalp EEG in juvenile myoclonic epilepsy, *NeuroImage Clin.* **22** (2019) 101759:1–10.
59. M. Arnold, W. H. Miltner, H. Witte, R. Bauer and C. Braun, Adaptive AR modeling of nonstationary time series by means of Kalman filtering, *IEEE Trans. Bio-med. Eng.* **45** (1998) 553–562.
60. G. Schwarz, Estimating the dimension of a model, *Ann. Stat.* **6** (1978) 461–464.
61. M. Campi, Performance of RLS identification algorithms with forgetting factor: A  $\Phi$ -mixing approach, *J. Math. Syst. Estim. Control* **4** (1994) 1–25.
62. B. T. T. Yeo, F. M. Krienen, J. Sepulcre, M. R. Sabuncu, D. Lashkari, M. Hollinshead, J. L. Roffman, J. W. Smoller, L. Zoller, J. R. Polimeni, B. Fischl, H. S. Liu and R. L. Buckner, The organization of the human cerebral cortex estimated by intrinsic functional connectivity, *J. Neurophysiol.* **106** (2011) 1125–1165.
63. J. D. Power, A. L. Cohen, S. M. Nelson, G. S. Wig, K. A. Barnes, J. A. Church, A. C. Vogel, T. O. Laumann, F. M. Miezin, B. L. Schlaggar and S. E. Petersen, Functional network organization of the human brain, *Neuron* **72** (2011) 665–678.
64. L. Z. Fan, H. Li, J. J. Zhuo, Y. Zhang, J. J. Wang, L. F. Chen, Z. Y. Yang, C. Y. Chu, S. M. Xie, A. R. Laird, P. T. Fox, S. B. Eickhoff, C. S. Yu and T. Z. Jiang, The human brainnetome atlas: A new brain atlas based on connectional architecture, *Cereb. Cortex* **26** (2016) 3508–3526.
65. L. Geerligs, R. N. Henson and Cam-CAN, Functional connectivity and structural covariance between regions of interest can be measured more accurately using multivariate distance correlation, *NeuroImage* **135** (2016) 16–31.
66. U. Ribary, S. M. Doesburg and L. M. Ward, Thalamocortical network dynamics: A framework for typical/atypical cortical oscillations and connectivity, in *Magnetoencephalography*, (Springer Berlin Heidelberg, Berlin, Heidelberg, 2014).
67. H. Blumenfeld and D. A. McCormick, Corticothalamic inputs control the pattern of activity generated in thalamocortical networks, *J. Neurosci.* **20** (2000) 5153–5162.
68. H. Adeli, S. Ghosh-Dastidar and N. Dadmehr, Alzheimer's disease: Models of computation and analysis of EEGs, *Clin. EEG Neurosci.* **36** (2005) 131–140.
69. N. Mammone, S. De Salvo, C. Ieracitano, S. Marino, A. Marra, F. Corallo and F. C. Morabito, A permutation disalignment index-based complex network approach to evaluate longitudinal changes in brain-electrical connectivity, *Entropy-Switz* **19** (2017) 548:1–15.
70. M. Ahmadlou, H. Adeli and A. Adeli, Graph theoretical analysis of organization of functional brain networks in ADHD, *Clin. EEG Neurosci.* **43** (2012) 5–13.
71. H. Adeli, S. Ghosh-Dastidar and N. Dadmehr, Alzheimer's disease and models of computation: Imaging, classification, and neural models, *J. Alzheimers Dis.* **7** (2005) 187–199.
72. M. Ahmadlou and H. Adeli, Complexity of weighted graph: A new technique to investigate structural complexity of brain activities with applications to aging and autism, *Neurosci. Lett.* **650** (2017) 103–108.
73. M. Kaminski and K. J. Blinowska, Directed transfer function is not influenced by volume conduction-independent pre-processing should be avoided, *Front. Comput. Neurosci.* **8** (2014) 61:1–3.
74. T. Yamanishi, J. Q. Liu and H. Nishimura, Modeling fluctuations in default-mode brain network using a spiking neural network, *Int. J. Neural Syst.* **22**(4) (2012) 1250016.
75. R. Scheeringa, K. M. Petersson, A. Kleinschmidt, O. Jensen and M. C. Bastiaansen, EEG alpha power modulation of fMRI resting-state connectivity, *Brain Connect.* **2** (2012) 254–264.
76. F. Sonmez, D. Atakli, H. Sari, T. Atay and B. Arpacı, Cognitive function in juvenile myoclonic epilepsy, *Epilepsy Behav.* **5** (2004) 329–336.
77. K. Culhane-Shelburne, L. Chapieski, M. Hiscock and D. Glaze, Executive functions in children with frontal and temporal lobe epilepsy, *Int. J. Neuropsych. Soc.* **8** (2002) 623–632.
78. S. Jiang, C. Luo, J. Gong, R. Peng, S. Ma, S. Tan, G. Ye, L. Dong and D. Yao, Aberrant thalamocortical connectivity in juvenile myoclonic epilepsy, *Int. J. Neural Syst.* **28**(1) (2018) 1750034.
79. P. R. Bauer, S. Kalitzin, M. Zijlmans, J. W. Sander and G. H. Visser, Cortical excitability as a potential clinical marker of epilepsy: A review of the clinical application of transcranial magnetic stimulation, *Int. J. Neural Syst.* **24**(2) (2014) 1430001.
80. A. L. Velasco, F. Velasco, M. Velasco, J. M. Nunez, D. Trejo and I. Garcia, Neuromodulation of epileptic foci in patients with non-lesional refractory motor epilepsy, *Int. J. Neural Syst.* **19** (2009) 139–147.
81. D. Martin-Lopez, D. Jimenez-Jimenez, L. Cabanes-Martinez, R. P. Selway, A. Valentin and G. Alarcon,

- The role of thalamus versus cortex in epilepsy: Evidence from human ictal centromedian recordings in patients assessed for deep brain stimulation, *Int. J. Neural Syst.* **27** (2017) 1750010.
82. C. Hamani, D. Andrade, M. Hodaie, R. Wennberg and A. Lozano, Deep brain stimulation for the treatment of epilepsy, *Int. J. Neural Syst.* **19** (2009) 213–226.
  83. C. Luo, Q. F. Li, Y. X. Lai, Y. Xia, Y. Qin, W. Liao, S. S. Li, D. Zhou, D. Z. Yao and Q. Y. Gong, Altered functional connectivity in default mode network in absence epilepsy: A resting-state fMRI study, *Human Brain Mapping* **32** (2011) 438–449.
  84. F. Moeller, M. Maneshi, F. Pittau, T. Gholipour, P. Bellec, F. Dubeau, C. Grova and J. Gotman, Functional connectivity in patients with idiopathic generalized epilepsy, *Epilepsia* **52** (2011) 515–522.
  85. M. Schreckenberger, C. Lange-Asschenfeld, M. Lochmann, K. Mann, T. Siessmeier, H. G. Buchholz, P. Bartenstein and G. Grunder, The thalamus as the generator and modulator of EEG alpha rhythm: A combined PET/EEG study with lorazepam challenge in humans, *NeuroImage* **22** (2004) 637–644.
  86. P. G. Larsson and H. Kostov, Lower frequency variability in the alpha activity in EEG among patients with epilepsy, *Clin. Neurophysiol.* **116** (2005) 2701–2706.
  87. C. Helmstaedter, B. Kemper and C. E. Elger, Neuropsychological aspects of frontal lobe epilepsy, *Neuropsychol.* **34** (1996) 399–406.
  88. B. Klugah-Brown, C. Luo, H. He, S. S. Jiang, G. K. Armah, Y. Wu, J. F. Li, W. J. Yin and D. Z. Yao, Altered dynamic functional network connectivity in frontal lobe epilepsy, *Brain Topogr.* **32** (2019) 394–404.
  89. T. R. Marshall, T. O. Bergmann and O. Jensen, Frontoparietal structural connectivity mediates the top-down control of neuronal synchronization associated with selective attention, *Plos Biol.* **13** (2015) e1002272:1–17.
  90. T. J. Buschman and E. K. Miller, Top-down versus bottom-up control of attention in the prefrontal and posterior parietal cortices, *Science* **315** (2007) 1860–1862.
  91. M. T. Hernandez, H. C. Sauerwein, I. Jambaque, E. De Guise, F. Lussier, A. Lortie, O. Dulac and M. Lassonde, Deficits in executive functions and motor coordination in children with frontal lobe epilepsy, *Neuropsychol.* **40** (2002) 384–400.
  92. N. Mammone, S. De Salvo, L. Bonanno, C. Ieracitano, S. Marino, A. Marra, A. Bramanti and F. C. Morabito, Brain network analysis of compressive sensed high-density EEG signals in AD and MCI subjects, *IEEE Trans. Ind. Inform.* **15** (2019) 527–536.
  93. N. Mammone, C. Ieracitano, H. Adeli, A. Bramanti and F. C. Morabito, Permutation Jaccard distance-based hierarchical clustering to estimate EEG network density modifications in MCI subjects, *IEEE Trans. Neural Netw. Lear* **29** (2018) 5122–5135.